

Parity nonconservation in nonradiative transitions in μ -mesic atoms

V. G. Gorshkov, A. I. Mikhailov, and A. N. Moskalev

Leningrad Institute of Nuclear Physics, USSR Academy of Sciences
(Submitted May 22, 1975)
Zh. Eksp. Teor. Fiz. 69, 1507-1516 (November 1975)

Nonradiative transitions in μ -mesic atoms involving the expulsion of shell electrons (Auger transitions) and the formation of electron-positron pairs are considered. It is shown that the weak interaction of the neutral currents leads to an asymmetry in the electron and positron emission with respect to the initial muon polarization. The asymmetry coefficient in the Auger transitions is 10^{-5} - 10^{-6} . The asymmetry coefficient in the pair production process can be increased by performing the measurements in the region of small resultant pair momenta.

PACS numbers: 36.10.+m, 32.10.Qy

1. INTRODUCTION

The existence of weak neutral currents^[1] leads to parity nonconservation in atomic processes^[2-4]. On account of the large μ -meson mass, the parity nonconservation phenomena should be most noticeable in μ -mesic atoms^[5-7]. It is generally suggested that, in order to observe parity nonconservation in radiative transitions, we can observe the highly forbidden, magnetic, one-photon transition from the excited 2S level to the ground 1S state, into which the weak interaction admixes the electric transition from the neighboring 2P level. The interference between the electric- and magnetic-transition amplitudes leads to the appearance of parity-nonconserving circular photon polarization, or to an asymmetry in the photon emission with respect to the initial μ -meson polarization ζ ^[5-7]. The degree of circular polarization or of asymmetry in the photon emission can attain in light μ -mesic atoms several percent^[5,6]. However, their observation is, for quite a number of reasons, complicated.

In particular, because of the relatively large P-level widths and the slow decrease of the Breit-Wigner distribution over energy, part of the unpolarized photons produced in the allowed 2P \rightarrow 1S transition will have the same frequency as the photons emitted in the 2S \rightarrow 1S transition under investigation. This can lead to a considerable effective decrease in the degrees of polarization and asymmetry if special measures are not taken. Such an obstacle can be avoided if, for example, we make use of the substantial difference in the lifetimes of the 2P and 2S states, and study the transitions from the metastable 2S levels after the population of the 2P levels have become nearly equal to zero.

The main difficulty encountered in the experimental study of the 2S \rightarrow 1S + γ transition is connected with the fact that the probability of this transition in light mesic atoms (where the parity nonconservation effects are especially pronounced) is small compared to the probability of the other possible transitions from the 2S state. On the other hand, in heavy mesic atoms, where the relation between the probabilities of the one-photon and other possible transitions is more favorable, the parity-nonconservation effects are comparatively small, being of the order of 10^{-4} - 10^{-5} .

In this paper we consider parity-nonconservation effects in nonradiative transitions in μ -mesic atoms. To them pertain Auger transitions involving the expulsion of one electron from the atom and transitions involving

	Z								
	3	4	5	8	23	25	27	30	40
ω/m	0.037	0.066	0.10	0.26	2.19	2.58	3.01	3.72	6.61
$w_{\gamma^+}, \text{sec}^{-1}$	30	5.3·10 ²	5.0·10 ³	5.5·10 ⁴	1.2·10 ⁶	2.4·10 ⁶	4.7·10 ⁶	1.1·10 ⁷	1.0·10 ⁷
$w_{2\gamma^+}, \text{sec}^{-1}$	1.2·10 ⁴	6.9·10 ⁴	2.7·10 ⁵	4.5·10 ⁶	1.4·10 ⁸	2.1·10 ⁸	2.9·10 ⁸	4.4·10 ⁸	1.2·10 ⁹
$w'_{\gamma^+}, \text{sec}^{-1}$	—	50	1.4·10 ⁴	2.8·10 ⁵	3.7·10 ⁶	8.4·10 ⁶	1.8·10 ⁷	4.8·10 ⁷	6.6·10 ⁷
F	—	—	—	—	—	—	—	—	—
$w_{\gamma^0}, \text{sec}^{-1}$	-1.6·10 ⁻⁷	4.4·10 ⁻⁷	2.0·10 ⁻⁷	1.3·10 ⁻⁷	1.1·10 ⁻⁷	1.1·10 ⁻⁷	1.2·10 ⁻⁷	1.2·10 ⁻⁷	1.3·10 ⁻⁷
$w_{\gamma^e}, \text{sec}^{-1}$	2.3·10 ⁴	2.3·10 ⁵	2.4·10 ⁶	2.7·10 ⁷	6.8·10 ⁸	7.7·10 ⁸	8.8·10 ⁸	1.1·10 ⁹	2.0·10 ⁹
$w_{\gamma^e}, \text{sec}^{-1}$	-4.6·10 ⁻⁴	1.3·10 ⁻³	5.6·10 ⁻³	3.5·10 ⁻²	2.2·10 ⁻¹	2.2·10 ⁻¹	2.2·10 ⁻¹	2.1·10 ⁻¹	1.8·10 ⁻¹
\mathcal{P}_e	—	—	—	—	1.0·10 ⁻⁴	2.5·10 ⁻⁴	1.1·10 ⁻⁴	4.5·10 ⁻⁴	5.8·10 ⁻⁴
\mathcal{P}_1	—	—	—	—	7.4·10 ⁻⁴	4.3·10 ⁻⁴	3.7·10 ⁻⁴	3.0·10 ⁻⁴	2.3·10 ⁻⁴

Note. The values of the asymmetry coefficients \mathcal{P}_e and \mathcal{P}_1 given correspond to $\kappa_p + N\kappa_n/Z = 1$. The radiative-transition probabilities and the mixing parameters F were taken from the papers^[4,7].

the production of electron-positron pairs. The Auger transition involving the transition of the μ meson from the 2S to the 1S level in the atom and accompanied by the expulsion of an electron from the 1S shell^[8] is the primary transition in μ -mesic atoms when the nuclear charge $Z \leq 10$. For $Z > 10$ the dominant mode becomes the one-quantum transition from the 2S to the 2P level. A significant role in mesic atoms is also played by the two-photon transition 2S \rightarrow 1S + 2γ . Pair production becomes possible at $Z > 22$, when the 2S \rightarrow 1S transition energy, $\omega = \frac{3}{8}m\mu(\alpha Z)^2$, begins to exceed 2m (m is the electron mass). The probability for pair production, w_{γ^+} , is, in contrast to the probability for the Auger effect, w_e , not limited by the phase volume of the initial bound electron. Therefore, w_{γ^+} rapidly outgrows w_e , and already at $Z = 27$ we have $w_{\gamma^+} > w_e$. A better idea about the relation between the probabilities of the different processes is given by the table. In it, besides the nonradiative transition probabilities w_e and w_{γ^+} , we give for comparison the probabilities for the transitions 2S \rightarrow 1S + γ (w_{γ^0}), 2S \rightarrow 1S + 2γ ($w_{2\gamma^+}$), and 2S \rightarrow 2P + γ (w'_{γ^+}).

Parity nonconservation in nonradiative transitions, as in radiative transitions, is connected with the interference of the two diagrams 1a and 1b, an interference which leads to the appearance in the electron emission of an asymmetry with respect to the initial μ -meson spin. The degree of asymmetry turns out to be proportional to the ratio of the amplitudes of the processes shown in Figs. 1b and 1a. The coefficient of mixing of the levels 2S and 2P, i.e., the product of the weak vertex W in Fig. 1b and the μ -meson propagator, which contains in the denominator the difference between the energies in the 2S and 2P_{1/2} states, is a quantity of the order of 10^{-7} , and weakly depends on Z ^[5-7]. The elec-

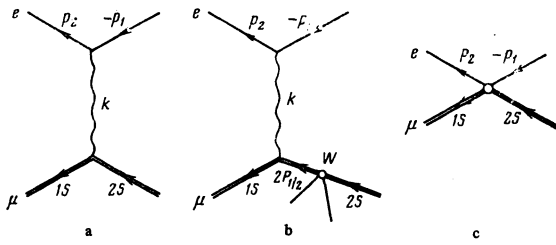


FIG. 1. Feynman diagrams for conversion processes.

tromagnetic transition shown in Fig. 1b is an E1 transition; therefore, it is intensified in comparison with the E0 and M1 transitions in Fig. 1a by a factor of $(qa_\mu)^{-1} = \eta_{\mu}/q$, where q is the momentum of the intermediate photon and $a_\mu = \eta_{\mu}^{-1} = (m_\mu \alpha Z)^{-1}$ is the Bohr radius for the μ meson. To sum up, the asymmetry coefficient \mathcal{P} turns out to be proportional to the quantity $\eta_{\mu}/q \times 10^{-7}$. For Auger transitions $q = p$, where p is the momentum of the outgoing electron. In the nonrelativistic region (for small Z), $p = (2m\omega)^{1/2}$, $\eta_{\mu}/q \sim (m_\mu/m)^{1/2}$, and $\mathcal{P} \sim 10^{-7} (m_\mu/m)^{1/2} \sim 10^{-6}$. In the relativistic region (for large Z), $q = p \sim \omega$, $\eta_{\mu}/q \sim (\alpha Z)^{-1}$, and $\mathcal{P} \sim 10^{-7} (\alpha Z)^{-1}$.

For transitions involving pair production when $Z > 22$, the momentum q of the intermediate photon is equal to the combined momentum of the pair and can be arbitrarily small, while the degree of asymmetry can theoretically be reduced to unity. Unfortunately, as q decreases, the differential probability for the process in Fig. 1a is $\sim q$, while the phase volume is $\sim q^2 dq$, so that for each order of magnitude earned in the asymmetry coefficient \mathcal{P} , we lose four orders of magnitude in the probability. In reality, we can, apparently, count in the pair-production process on a value for \mathcal{P} not greater than 10^{-5} .

Another mechanism leading to parity-nonconserving correlations and not connected with the mixing of the 2S and 2P levels is also possible in nonradiative transitions in mesic atoms. This is the weak direct contact interaction between the electron and muon currents (see Fig. 1c). The ratio of the magnitude of this diagram to that of the diagram in Fig. 1a is of the order of $Gq^2/4\pi\alpha \sim 10^{-11}$, where G is the Fermi weak-interaction constant. For the processes under consideration, on account of the smallness of q , Fig. 1c is four-five orders of magnitude smaller than Fig. 1b, and therefore we shall not consider it.

The M1 magnetic transition in Fig. 1a is highly forbidden, and arises only when the retardation of the spin-orbit interaction is allowed for^[8-10]. The magnitude of the M1 term is of order $(\alpha Z)^2$ times the magnitude of the E0 term; therefore, we shall neglect the magnetic transition. It should, however, be noted that the interference of the M1 and E1 transitions can lead to another P-odd correlation, i.e., to the longitudinal polarization of the final electrons (positrons), a polarization which is absent when only the E0-E1 interference is taken into account. It follows from the foregoing that the longitudinal polarization is $(\alpha Z)^2$ times less than the degree of asymmetry \mathcal{P} in the electron emission with respect to the initial μ -meson polarization.

Furthermore, the magnetic term is responsible for the appearance of a parity-conserving correlation of the type $(\xi_\mu \cdot \mathbf{q})(\xi_e \cdot \mathbf{q})$ (where $\xi_\mu/2$ and $\xi_e/2$ are the μ -

meson and electron spins), which vanishes upon averaging over the electron spins. The relative contribution of this correlation $\sim (\alpha Z)^2$, which is much greater than the asymmetry \mathcal{P} connected with parity nonconservation. Therefore, when the averaging over the final-electron spins ξ_e is not sufficiently thorough, the indicated correlation can imitate the P-odd asymmetry $(\xi_\mu \cdot \mathbf{q})$. For the pair-production process, when we take into account the exchange of two quanta one of which is of multipole order M1, there also arises the azimuthal asymmetry $\xi_\mu \cdot [\mathbf{p}_1 \times \mathbf{p}_2]$ (\mathbf{p}_2 and \mathbf{p}_1 are the electron and positron momenta), the relative contribution of which is proportional to $(\alpha Z)^3$. The azimuthal asymmetry can also hinder the measurement of the asymmetry connected with weak interactions.

There may arise in the experimental study of non-radiative transitions the difficulty mentioned above in connection with radiative transitions. Because of the small energy difference between the 2P and 2S states, it is difficult to separate, according to energy, the conversion electrons connected with the 2S \rightarrow 1S transition from the background electrons connected with the 2P \rightarrow 1S transition. In the case of nonradiative transitions the influence of this background is of less importance, since the probability of the nonradiative 2P \rightarrow 1S transition is greater than the probability of the 2S \rightarrow 1S transition by a factor of only $\sim 10^2$ (and not by a factor of $\sim 10^{14}Z^{-6}$, as in the case of the one-photon transitions). The background can also be suppressed through the use of the difference in lifetimes of the 2P and 2S states.

In computing the amplitudes of the nonradiative transitions, we did not take the finite dimensions of the nucleus into account. For light mesic atoms the corrections for the finite nuclear dimensions are of the order of $qR_N \sim \eta_{\mu}/m_\mu \sim (\alpha Z)m_\mu/m_\pi \sim \alpha Z$, and can be discarded in our approximation. For mesic atoms with large Z , where these corrections are more important, the obtained results should be regarded as approximate estimates.

2. THE AMPLITUDE OF THE PROCESSES

The Auger-transition and pair-production amplitude can be obtained from the diagrams in Figs. 1a and 1b. In the momentum representation the amplitude has the simplest form—the products of the muon $J(\mathbf{q})$ and electron $J'(\mathbf{q})$ currents with the photon propagator $1/k^2$:

$$A = \int J_\nu(\mathbf{q}) \frac{4\pi\alpha}{k^2} J'_\nu(\mathbf{q}) \frac{d^3\mathbf{q}}{(2\pi)^3}, \quad k^2 = \omega^2 - \mathbf{q}^2, \quad \alpha = 1/137, \quad (1)$$

$$J_\nu(\mathbf{q}) = \int \bar{\Psi}_f(\mathbf{r}) \gamma_\nu \Psi_i(\mathbf{r}) e^{-i\mathbf{q}\cdot\mathbf{r}} d^3\mathbf{r}. \quad (2)$$

In the zeroth approximation in the Coulomb field, at the electron vertex in Fig. 1, momentum is conserved and the current $J'_\nu(\mathbf{q})$ can be represented in the form

$$J'_\nu(\mathbf{q}) = j_\nu(\mathbf{q}) (2\pi)^3 \delta(\mathbf{q} - \mathbf{p}_1 - \mathbf{p}_2). \quad (3)$$

Substituting this expression into (1), we obtain

$$A = J_\nu(\mathbf{q}) \frac{4\pi\alpha}{k^2} j_\nu(\mathbf{q}). \quad (4)$$

For the Auger effect

$$\begin{aligned} \mathbf{p}_1 = 0, \quad \mathbf{p}_2 = \mathbf{p} = \mathbf{q}, \quad j_\nu(\mathbf{q}) = N_1 \bar{u}_p \gamma_\nu u_0, \\ N_1^2 = \eta^2/\pi, \quad \eta = m\alpha Z, \quad N_1 = \Psi_{1s}^*(0), \end{aligned} \quad (5a)$$

where u_p, u_0 are the Dirac bispinors and N_1 is the

normalization factor for the wave function of the electron in the initial state, the square of which performs the function of the phase volume of the 1S electron. For pair production

$$j_+(\mathbf{q}) = \bar{u}_{p_1} \gamma_{\mu} u_{-p_1}, \quad \mathbf{q} = \mathbf{p}_1 + \mathbf{p}_2. \quad (5b)$$

It is convenient to write the expression for the muon current in the lowest approximation in αZ in a two-component form. Using the expression for the coefficient of mixing of the 2S and 2P states^[5-7]:

$$iF = \frac{\langle 2P_{1/2} | W | 2S \rangle}{\omega_L} = i \frac{G m_{\mu}^2}{32\pi} \left(\frac{3}{2} \right)^{1/2} (\alpha Z)^3 \frac{\eta_{\mu}}{\omega_L} (Z \kappa_p + N \kappa_n), \quad (6)$$

$$\eta_{\mu} = m_{\mu} \alpha Z, \quad \omega_L = E(2S) - E(2P_{1/2}),$$

where G is the Fermi weak-interaction constant, κ_p and κ_n are the coupling constants for neutral currents for protons and neutrons, we obtain the following expression for the muon current $J_{\nu}(\mathbf{q})$ (Fig. 1b):

$$J_0 = 4\sqrt{2} \left(\frac{\alpha Z}{9} \right)^2 \frac{q^2}{\omega^2} \chi_{1s} \cdot \left\{ 1 + \sigma \times \mathbf{n} \frac{\Lambda}{q} \right\} \chi_{2s}, \quad (7)$$

$$\mathbf{J} = 4\sqrt{2} \left(\frac{\alpha Z}{9} \right)^2 \frac{q}{\omega} \chi_{1s} \cdot \left\{ \mathbf{n} + \sigma \frac{\Lambda}{q} - e[\sigma \times \mathbf{n}] \frac{\omega}{m_{\mu}} \left(1 + \frac{k^2}{2m_{\mu}\omega} \right) \right\} \chi_{2s}.$$

Here

$$\omega = E(2S) - E(1S) = \frac{3}{8} m_{\mu} (\alpha Z)^2, \quad \mathbf{n} = \mathbf{q}/q, \quad (8)$$

$$\Lambda = \frac{\sqrt{3}}{2} \eta_{\mu} F = F \sqrt{2} m_{\mu} \omega = \alpha Z \frac{G m_{\mu}^2}{3\pi \sqrt{2}} \frac{\omega^2}{\omega_L} (Z \kappa_p + N \kappa_n),$$

$$k = (\omega, \mathbf{q}), \quad k^2 = \omega^2 - q^2,$$

χ_i and σ are the Pauli spinors and matrices. The first terms in J_0 and \mathbf{J} correspond to the E0 transition; the second terms, containing Λ , to the E1 transition. We have also written out the magnetic M1 term (the last term in \mathbf{J}), which is of the order of $\omega/m_{\mu} = \frac{3}{8} (\alpha Z)^2$ as compared to the E0 part of the current. The magnetic term is necessary for the estimation of the degree of longitudinal polarization of the final electrons, as well as of the correlations that hinder the observation of the parity-nonconservation effects and that were mentioned in the Introduction. In computing the asymmetry in the electron or positron emission, we can neglect this term. It can be seen directly that the current (7) satisfies the transversality condition

$$kJ = \omega J_0 - q\mathbf{J} = 0.$$

The probability for the production of the pair e^+e^- can be computed with the aid of the formula

$$d\omega = \sum_{\mu, \epsilon} |A|^2 d\Gamma = \left(\frac{4\pi\alpha}{k^2} \right)^2 S_{p_1} S_{p_2} \{ (\hat{p}_1 + m) \hat{J} (\hat{p}_1 - m) \rho_{\mu} \hat{J} \} d\Gamma, \quad (9)$$

$$\rho_{\mu} = \frac{1}{2} (1 + \xi \sigma),$$

$$d\Gamma = \frac{d^3 p_1}{2\epsilon_1 (2\pi)^3} \frac{d^3 p_2}{2\epsilon_2 (2\pi)^3} 2\pi \delta(\omega - \epsilon_1 - \epsilon_2),$$

$$\hat{a} = a_{\mu} \gamma_{\mu},$$

where \mathbf{p}_1 , ϵ_1 and \mathbf{p}_2 , ϵ_2 are the momentum, energy of the positron and electron, ρ_{μ} is the polarization density matrix of the μ meson, and $\xi/2$ is the mean value of the initial muon spin. To compute the probability for the Auger effect in (9), we should set

$$p_1 = 0, \quad \epsilon_1 = -m, \quad (2\pi)^{-3} d^3 p_1 = N_1^2. \quad (10)$$

The computation of the trace with respect to the muon variables with the density matrix ρ_{μ} is equivalent to the replacement of the σ matrix in the muon currents

(7) by ξ and the dropping of the Pauli spinors χ_i (the terms quadratic in σ in the product of the muon currents in (9) are of the order of G^2 , and should be discarded). The computation of the trace with respect to the electron variables yields

$$d\omega = \left(\frac{4\pi\alpha}{k^2} \right)^2 4 \{ 2 \operatorname{Re} (p_2 J) (p_1 J^*) - (p_1 p_2 + m^2) (J J^*) \} d\Gamma. \quad (11)$$

3. THE PROBABILITY OF THE AUGER EFFECT

Carrying out the substitutions (10) in the formula (11), we obtain

$$d\omega_e = \omega_e (1 + \mathcal{P}_e \xi \mathbf{n}) \frac{d\Omega_{\mathbf{n}}}{4\pi},$$

$$\omega_e = m \alpha^2 \frac{2^{21} \sqrt{3}}{3^{12}} \left(\frac{m}{m_{\mu}} \right)^{3+1/2} \left(1 + \frac{\omega}{2m} \right)^{1/2}, \quad (12)$$

$$\mathcal{P}_e = 2F \sqrt{\frac{m_{\mu}}{m}} \frac{1}{(1 + \omega/2m)^{1/2}}, \quad \omega = \frac{3}{8} m_{\mu} (\alpha Z)^2, \quad \mathbf{n} = \frac{\mathbf{p}}{p},$$

where F is defined in (6) and \mathbf{p} is the momentum of the outgoing electron. In the nonrelativistic approximation, in which $\omega \ll 2m$ ($Z \ll 22$), we can replace $(1 + \omega/2m)$ in (12) by unity. In this approximation, only the temporal (Coulomb) part of the current (7) makes a contribution to the probability (12). The results of the calculations of the total Auger-transition probability w_e and of the degree of asymmetry \mathcal{P}_e for mesic atoms with different Z are presented in the Table, where we also indicate the values of the coefficients F of mixing of the 2S and 2P states that were used in the calculations^[5-7]. The greatest asymmetry $\mathcal{P}_e \sim 10^{-5}$ can be expected in mesic atoms of Li and Be (because of the large coefficient of mixing of the 2S and 2P levels); for other mesic atoms the quantity $\mathcal{P}_e \sim (2-5) \times 10^{-6}$. In spite of the small magnitude of the parity-nonconservation effects, as compared to the radiative transitions, Auger transitions in light mesic atoms may be of interest because of their high probability.

4. PAIR PRODUCTION

For the pair-production process the formula (11) gives

$$d\omega_{e^+e^-} = (8\pi\alpha)^2 \left(\frac{2}{9} \frac{\alpha Z}{\omega} \right)^4 \left\{ q^2 - \epsilon^2 + 2\Lambda \xi \left[\mathbf{p}_1 \left(1 + \frac{2\epsilon_1 \epsilon}{k^2} \right) + \mathbf{p}_2 \left(1 - \frac{2\epsilon_1 \epsilon}{k^2} \right) \right] \right\} d\Gamma, \quad (13)$$

$$\mathbf{q} = \mathbf{p}_1 + \mathbf{p}_2, \quad \epsilon = \epsilon_2 - \epsilon_1, \quad k^2 = \omega^2 - q^2, \quad \omega = \epsilon_1 + \epsilon_2.$$

The phase volume $d\Gamma$ and the quantity Λ are defined in the formulas (9) and (8).

In the presence of an initial muon polarization ξ , the final state of the pair e^+e^- is characterized by three independent variables. As these variables we can choose q , ϵ_1 , and the angle φ_1 between the vectors ξ and \mathbf{p}_1 (Fig. 2a) or the angle φ between the vectors ξ and \mathbf{q} (Fig. 2b). The angles φ_1 and φ , as can be seen from Fig. 2, vary within the usual limits $0 \leq \varphi, \varphi_1 \leq \pi$. The physical region in the variables q and ϵ_1 are limited by the condition

$$|p_1 - q| \leq p_2 \leq p_1 + q, \quad p_1^2 = \epsilon_1^2 + m^2, \quad \epsilon_1 + \epsilon_2 = \omega.$$

This region is hatched in Fig. 3. The upper and lower boundaries of the physical region are determined by the equation

$$\epsilon_1 = \frac{\omega \pm \gamma q}{2}, \quad \gamma = \left(1 - \frac{4m^2}{k^2} \right)^{1/2}, \quad k^2 = \omega^2 - q^2.$$

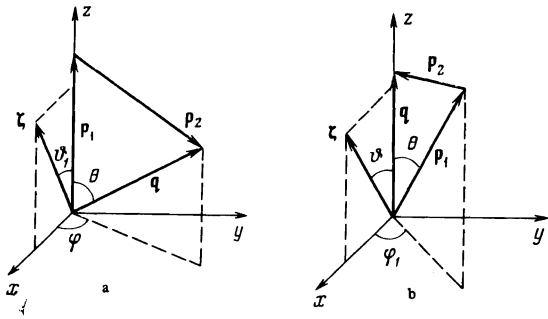


FIG. 2. Kinematic variables in the e^+e^- pair production reaction.

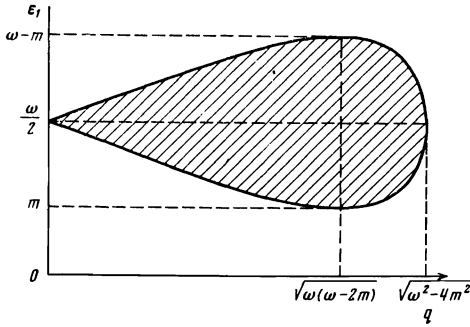


FIG. 3. The physical region for the e^+e^- pair production process.

The maximum and minimum values of ϵ_1 are attained at $q = \sqrt{\omega(\omega - 2m)}$. The maximum value of q is attained at $\epsilon_1 = \omega/2$, and is equal to

$$q = q_m = (\omega^2 - 4m^2)^{1/2}.$$

The measurement of the momentum q transferred to the mesic atom is possible only when the electron and positron momenta are also measured at the same time; for the direct measurement of the recoil of the mesic atom is very complicated. If only the positrons are detected in the experiment, the formula (13) for the probability should be integrated over all q . Using the coordinate axes shown in Fig. 2a, and taking into account the equalities

$$d^3p_2 = d^3q = q^2 dq d\varphi d\cos\theta, \quad d^3p_1 = p_1 \epsilon_1 d\epsilon_1 d\varphi_1 d\cos\theta_1,$$

we remove in $d\Gamma$ the energy δ -function by integrating over $\cos\theta = \mathbf{q} \cdot \mathbf{p}_1 / qp_1$. Rewriting in (13) the vector \mathbf{p}_2 in the form $\mathbf{q} - \mathbf{p}_1$ and averaging over the angle φ (Fig. 2a), we obtain

$$\overline{\zeta \mathbf{q}} = \int \zeta \mathbf{q} \frac{d\varphi}{2\pi} = (\zeta \mathbf{n}_1) (q \mathbf{n}_1),$$

$$\mathbf{n}_1 = \frac{\mathbf{p}_1}{p_1}, \quad q \mathbf{n}_1 = \frac{q^2 - \omega \epsilon_1}{2p_1}.$$

Integrating further over q at fixed ϵ_1 (Fig. 3), we obtain the distribution over ϵ_1 and $t_1 = \zeta \cdot \mathbf{n}_1 / \zeta = \cos\vartheta_1$:

$$dw_{+-}(\epsilon_1, t_1) = \frac{8\alpha^2}{\pi} \left(\frac{2\alpha Z}{9\omega} \right)^4 p_2 p_1 (\epsilon_2 \epsilon_1 - m^2) \{1 + \zeta \mathbf{n}_1 \mathcal{P}_1(\epsilon_1)\} d\epsilon_1 dt_1,$$

$$\mathcal{P}_1(\epsilon_1) = \frac{\Lambda}{p_1} \left\{ 1 - \frac{m^2 \epsilon \omega}{p_2 p_1 (\epsilon_2 \epsilon_1 - m^2)} \ln \frac{m^2 + \epsilon_2 \epsilon_1 + p_2 p_1}{m\omega} \right\}. \quad (14)$$

For $p_1 \rightarrow 0$ the expression in the curly brackets in the expression for $\mathcal{P}_1(\epsilon_1)$ is proportional to p_1^2 , and the asymmetry coefficient tends to zero linearly in p_1 . At the opposite edge of the spectrum, i.e., for $p_2 \rightarrow 0$ and $p_1 \rightarrow p_{1 \max} = \sqrt{\omega(\omega - 2m)}$, the asymmetry $\mathcal{P}_1(\epsilon_1) \rightarrow 2\Lambda/p_{1 \max} = 2\Lambda[\omega(\omega - 2m)]^{-1/2}$. The diagrams il-

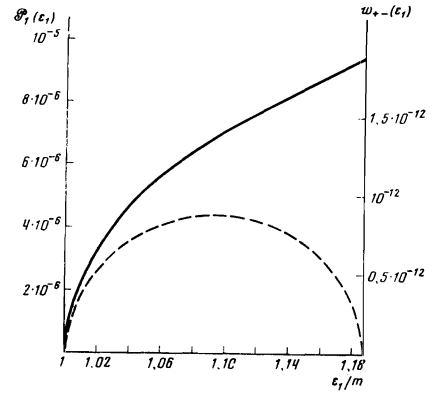


FIG. 4. Dependence of the asymmetry coefficient $\mathcal{P}_1(\epsilon_1)$ (solid curve) and of the pair production probability $w_{+-}(\epsilon_1)$ (dashed curve) on the positron energy ϵ_1 for mesic atoms with $Z = 23$.

lustrating the dependence of \mathcal{P}_1 on the positron energy ϵ_1 and the energy distribution of the positrons for mesic atoms with $Z = 23$ are shown in Fig. 4.

If we fix only the direction \mathbf{n}_1 of positron emission independently of its energy, then the angular distribution of the positrons can be obtained from (14) by integrating it over ϵ_1 :

$$dw_{+-}(t_1) = \int w_{+-} \{1 + \zeta \mathbf{n}_1 \mathcal{P}_1\} dt_1. \quad (15)$$

Numerical values of the total pair-conversion probability w_{+-} and of the asymmetry coefficient \mathcal{P}_1 are presented in the Table. An analytic expression for w_{+-} is given below (the formula (20)). In the nonrelativistic approximation, in which $\omega - 2m \equiv \epsilon_0 \ll m$, the formulas (14) and (15) assume the simple form:

$$dw_{+-}(\epsilon_1, t_1) = \frac{8\alpha^2}{\pi} \left(\frac{\alpha Z}{9} \right)^4 \frac{\epsilon_0 p_2 p_1}{m^3} \{1 + \zeta \mathbf{n}_1 \mathcal{P}_1(\epsilon_1)\} d\epsilon_1 dt_1, \quad (14a)$$

$$\mathcal{P}_1(\epsilon_1) = \Lambda p_1 / m \epsilon_0, \quad p_2 = (2m\epsilon_0 - p_1^2)^{1/2}.$$

Integration of (14a) over ϵ_1 yields

$$dw_{+-}(t_1) = 2\alpha^2 (\alpha Z / 9)^4 m (\epsilon_0 / m)^3 \{1 + \zeta \mathbf{n}_1 \mathcal{P}_1\} dt_1,$$

$$\mathcal{P}_1 = \frac{64}{15\pi} \frac{\Lambda}{(2m\epsilon_0)^{1/2}}, \quad \epsilon_0 = \omega - 2m. \quad (15a)$$

It can be seen from (15a) that the coefficient of asymmetry grows, as the reaction threshold is approached, in proportion to $q_m^{-1} \propto (2m\epsilon_0)^{-1/2}$, while the probability decreases in proportion to ϵ_0^3 .

During the simultaneous measurement of the electron and positron momenta, we can measure the asymmetry with respect to the resultant pair momentum q . The differential probability in these variables assumes, after averaging over the angle φ_1 (see Fig. 2b), the especially simple form:

$$dw_{+-}(q, \epsilon_1, t) = \frac{2\alpha^2}{\pi} \left(\frac{2\alpha Z}{9\omega} \right)^4 (q^2 - \epsilon^2) \left\{ 1 + 2\zeta \mathbf{n} \frac{\Lambda}{q} \right\} q dq d\epsilon_1 dt, \quad (16)$$

$$t = \cos\vartheta = \zeta \mathbf{n} / \zeta.$$

Integrating (16) over ϵ_1 , we obtain

$$dw_{+-}(q, t) = \int w_{+-}(q) \{1 + \zeta \mathbf{n} \mathcal{P}(q)\} dq dt, \quad (17)$$

where

$$w_{+-}(q) = \frac{8\alpha^2}{3\pi} \left(\frac{2\alpha Z}{9\omega} \right)^4 q^4 \left(1 + \frac{2m^2}{k^2} \right) \left(1 - \frac{4m^2}{k^2} \right)^{1/2},$$

$$\mathcal{P}(q) = 2\Lambda/q. \quad (18)$$

The linear growth of the asymmetry coefficient $\mathcal{P}(q)^2$ with decreasing q can clearly be seen from the formu-

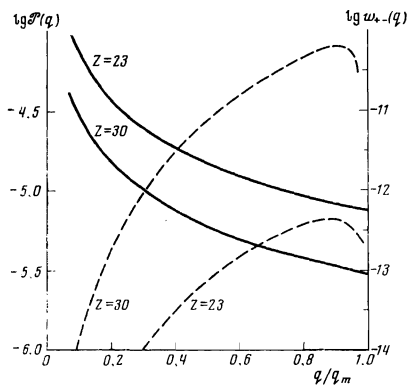


FIG. 5. Dependence of the asymmetry coefficient $\mathcal{P}(q)$ (solid curve) and of the pair production probability $w_{+-}(q)$ (dashed curve) on the pair momentum q for mesic atoms with $Z = 23, 30$. Along the horizontal are plotted the values of q/q_m , where $q_m = (\omega^2 - 4m^2)^{1/2}$ is the maximum possible momentum of the e^+e^- pair.

las (16) and (18); in this case, however, the pair-production probability decreases rapidly in proportion to q^4 . An idea about the scale of these quantities is given by Fig. 5. Integrating (17) over q , we obtain an angular distribution of the form

$$dw_{+-}(t) = \frac{1}{2} w_{+-} \{1 + \zeta n \mathcal{P}\} dt, \quad (19)$$

where the total pair-production probability w_{+-} and the asymmetry coefficient \mathcal{P} are expressible in terms of the hypergeometric functions ${}_2F_1$ according to the formulas

$$w_{+-} = 2\alpha^2 \left(\frac{\alpha Z}{q}\right)^4 \left(\frac{q_m}{\omega}\right)^5 q_m {}_2F_1\left(\frac{1}{2}, \frac{3}{2}; 4; x\right),$$

$$\mathcal{P} = \frac{2^7 \Lambda}{15\pi q_m} \frac{{}_2F_1(1/2, 1; 7/2; x)}{{}_2F_1(1/2, 3/2; 4; x)} \quad (20)$$

$$q_m = (\omega^2 - 4m^2)^{1/2}, \quad x = q_m^2/\omega^2 = 1 - 4m^2/\omega^2.$$

In the nonrelativistic limit the formula (19) assumes a form similar to (15a) with $\mathcal{P} = \mathcal{P}_1 \sqrt{2}$.

The authors are grateful to N. P. Popov for a discussion of the work.

¹The probability of Auger transitions involving the expulsion of electrons from the 1S shell constitutes 80% of the total probability of Auger transitions from all the shells because of the decrease of the phase volume of the bound electrons in proportion to n^{-3} , where n is the principal quantum number.

²If we obtain a distribution of the type (17) in the mixed variables (q, t) of Fig. 2a, then the asymmetry coefficient $\mathcal{P}_1(q)$ characterizing the correlation ζn , will no longer be singular at $q \rightarrow 0$.

¹F. J. Hasert et al., Phys. Lett. B46, 138 (1973).

²Ya. B. Zel'dovich, Zh. Eksp. Teor. Fiz. 36, 964 (1959) [Sov. Phys. JETP 9, 682 (1959)].

³F. C. Michel, Phys. Rev. B138, 408 (1965).

⁴A. N. Moskalev, Pis'ma Zh. Eksp. Teor. Fiz. 19, 229 (1974) [JETP Lett. 19, 141 (1974)].

⁵A. N. Moskalev, Pis'ma Zh. Eksp. Teor. Fiz. 19, 394 (1974) [JETP Lett. 19, 216 (1974)].

⁶J. Bernabeu, T. E. O. Ericson, and C. Jarlskog, Phys. Lett. B50, 467 (1974).

⁷G. Feinberg and M. Y. Chen, Phys. Rev. D10, 190 (1974).

⁸G. Breit and E. Teller, Astrophys. J. 91, 215 (1940).

⁹V. Ch. Zhukovskiĭ, M. M. Kolesnikova, A. A. Sokolov, and I. Kherrmann, Opt. Spektrosk. 28, 622 (1970) [Opt. Spectrosc. 28, 337 (1970)].

¹⁰C. Drake, Phys. Rev. A3, 908 (1971).

Translated by A. K. Agyei
163